https://doi.org/10.1007/s41230-018-8086-2

Distribution of SiC particles in semisolid electromagnetic-mechanical stir-casting Al-SiC composite

Yun-hui Du, *Peng Zhang, Wei-yi Zhang, and Yu-jie Wang

School of Mechanical, Electronic and Control Engineering, Beijing Jiaotong University, Beijing 100044, China

Abstract: The distribution of SiC particles in Al-SiC composite can greatly influence the mechanical performances of Al-SiC composite. To realize the homogeneous distribution of SiC particles in stir-casting Al-SiC composite, semisolid stir casting of Al-4.25vol.%SiC composite was conducted using a special electromagnetic-mechanical stirring equipment made by our team, in which there are three uniformly-distributed blades with a horizontal tilt angle of 25 ° to mechanically raise the SiC particles by creating an upward movement of slurry under electromagnetic stirring. The microstructure of the as-cast Al-SiC composites was observed by Scanning Electron Mcroscopy (SEM). The volume fraction of SiC particles was measured by image analysis using the Quantimet 520 Image Processing and Analysis System. The tensile strength of the Al-4.25vol.%SiC composites was measured by tensile testing. Results show that the Al-4.25vol.%SiC composites with the homogeneous distrbutin of SiC particles can be obtained by the electromagnetic-mechanical stirring casting with the speed of 300 and 600 r·min^{-1} at 620 °C. The differences between the volume fraction of SiC particles at the top of ingot and that at the bottom are both ~0.04vol.% with the stirring speed of 300 and 600 r·min^{-1}, which are so small that the distribution of SiC particles can be seen as the homogeneous. The tensile strength of the Al matrix is enhanced by 51.2% due to the uniformly distributed SiC particles. The porosity of the composite mainly results from the solidification shrinkage of slurry and it is less than 0.04vol.%.

Key words: Al-SiC composite; stir casting; particle distribution; microstructure; performance

CLC numbers: TG146.21 **Document code:** A **Article ID:** 1672-6421(2018)05-351-07

Al-SiC composite is made up of Al matrix and SiC particles [1]. Al matrix includes pure Al and Al alloys. SiC particle is a kind of brittle and hard phase and is used to improve the mechanical property of Al matrix. Therefore, Al-SiC composites possess performance qualities both metals and ceramics such as excellent specific strength, large specific stiffness, high thermal conductivity, low coefficient of thermal expansion, outstanding damping property, superior abradability, good fatigue resistance, etc., and the Al-SiC composites are widely used in automotive, aerospace, optical and electronic packaging fields [2–5].

Among the processing technologies of Al-SiC composite [6–9], stir casting, which mainly involves the stirring of Al-SiC slurry and the casting of composite, is considered as one of the most economical and simplest processing technologies for Al-SiC composites. Nevertheless, there is a vital problem in the stir-casting of Al-SiC composite, i.e. the uneven distribution of SiC particles, which can greatly degrade the mechanical properties of composite [10–11].

Many studies have been conducted on ameliorating the distribution of SiC particles in Al-SiC composites by improving the wettability of SiC particle to Al matrix and restraining the settling of SiC particles during casting [10, 12–16]. Ureña et al. enhanced the wettability of SiC particles via oxidation treatment of SiC particles [12]. Singh [13], León [14] and Vanarotti [15] et al. ameliorated the wettability of SiC particles using MgO and $MgAl_2O_4$ coatings, nickel coating and copper coating on SiC particles, respectively. Naher [10] and Hashim[16] et al. hampered the settling of SiC particles by means of semi-solid technique and quick solidification process.

It can be inferred that the advanced Al-SiC composite with a good performance would be obtained if the homogeneous distribution of SiC particles could be

***Yun-hui Du**

Female, born in 1969, professor. She has been working in the field of composites. Her research focuses on new materials and new technologies. Her academic research has lead to the publication of more than 80 papers.

E-mail: yhdu@bjtu.edu.cn

Received: 2018-07-13; Accepted: 2018-08-05

realized during the stirring process, and the settling of SiC particles could be restrained during the casting process. In this work, a special electromagnetic-mechanical stirring equipment made by our team was used to stir the Al-SiC slurry, and the Al-SiC ingot was cast by the semisolid permanent mold casting. Moreover, the tensile properties of the homogeneous Al-SiC composite were measured.

2 Experimental

2.1 Materials

Al-1.5wt.%Si aluminum alloy with a solid-liquid temperature range of 580–650 °C, which is fit for semi-solid casting, was used as the Al matrix. The 625-mesh black SiC particles with an average size of 20 μm, which did not undergo any additional treatment, were used as the reinforced particles, and the volume fraction of SiC particles was 4.25vol.%.

2.2 Electromagnetic-mechanical stirring equipment

The electromagnetic-mechanical stirring equipment of Al-4.25vol.%SiC slurry is shown in Fig. 1. A 25 kW electromagnetic stirrer with an encloser was used to stir the slurry. The Φ100 mm stainless steel crucible was fixed on the shelf. On the inner wall of crucible, a screw thread (Fig. 2) was lathed, by which the threaded cover is screwed into the crucible. Three blades with the size of 45 mm × 30 mm and a horizontal tilt angle of 25 °, which can create an upward movement of slurry to mechanically raise the SiC particles under electromagnetic stirring (Fig. 3), were uniformly distributed on the inner wall of crucible. The sealing plug on the threaded cover was used to separate the slurry from the atmosphere. Three cooling pipes and three heating rods, arranging evenly and alternately on the crucible wall, were respectively controlled by the external power and coolant supply system to make sure the temperature of slurry was stable at a certain temperature. The thermocouple was sealed on the stainless steel threaded cover to monitor the slurry temperature. The blockage was adopted to pour out the slurry. Motor 1, transmission gear 1 and sliding plate 1, installed on the mounting plate, were employed to realize the up-and-down movement of the threaded cover along the sliding groove. Torque motor 2 and transmission gear 2, mounted on the sliding plate 2, were applied to actualize the rotary movement of the threaded cover. The elastic connector was utilized to achieve the flexible contact between the threaded cover and the crucible.

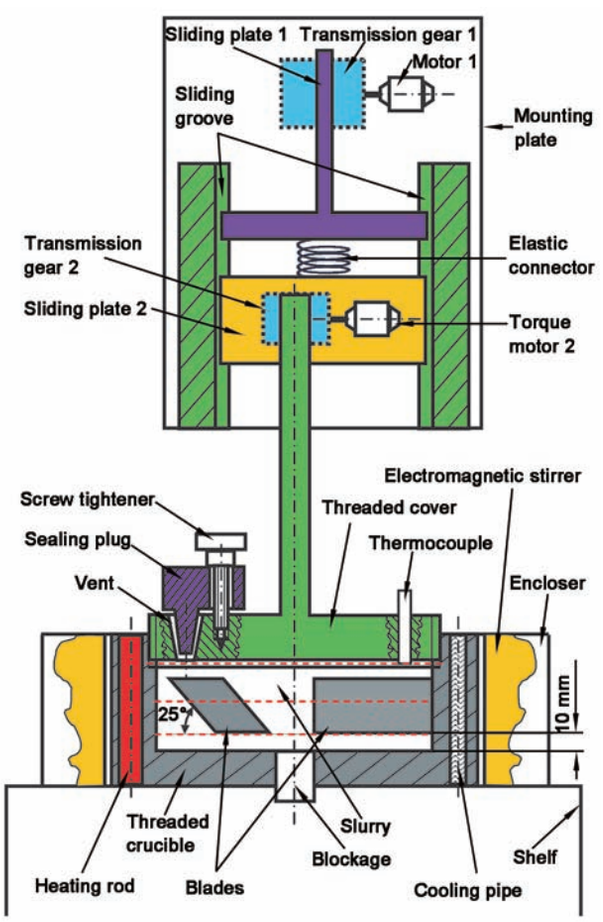

Fig. 1: Electromagnetic-mechanical stirring equipment in present work

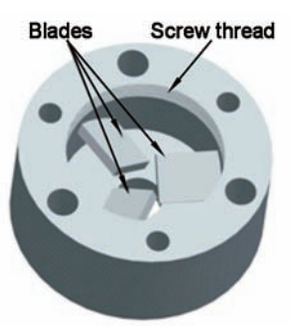

Fig. 2: Crucible with screw thread and blades

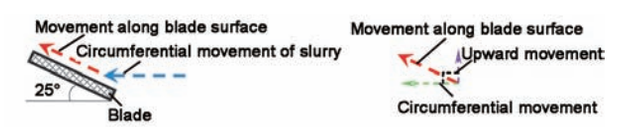

Fig. 3: Influence of horizontal tilt angle 25° on movement of slurry: (a) change of slurry movement; (b) decomposition of movement along blade surface

2.3 Procedures

The procedures and the conditions to prepare the Al-4.25vol.% SiC composite were as follows:

(1) Preparing Al-1.5wt%Si liquid, the temperature of which was held at 700 °C after degassing.

(2) Pouring the above liquid on the 625-mesh black SiC particles wrapped in Al foil at the bottom of the crucible which was preheated to the temperature of 600 °C by the heating rods in the wall of the crucible.

(3) Switching on the motor 1 to lower the threaded cover to the screw thread on the inner wall of the crucible top. Switching off the motor 1 and switching on the torque motor 2 to screw the threaded cover into the crucible to force out the air.

(4) Switching off the torque motor 2 as soon as the liquid coming out of the vent and screwing down the screw tightener to seal the vent by the sealing plug.

(5) Switching on the electromagnetic stirrer and adjusting the temperature of the liquid to 620 °C by controlling the cooling pipes and the heating rods with the monitoring of thermocouple.

Meanwhile, switching on the torque motor 2 to ceaselessly screw the threaded cover into the crucible in agreement with the cooling shrinkage of the melt with a constant torque. The electromagnetic stirring speed was 300, 600 and 900 r·min^{-1} and the temperature precision was ±1 °C. In addition, the stirring temperature of 635 °C and the sirring speed of 600 r·min^{-1} were carried out for preparing the refernce ingot to compare the effects of the differnt volume fraction of primary solid Al particles on the distribution of SiC particles.

(6) Switching off the electromagnetic stirrer 10 minutes later and unscrewing the screw tightener. Pulling out the blockage and pouring the slurry into a permanent mold to cast the *Φ*50 mm ×100 mm ingot of Al-SiC composite. The cooling rate of the permanent mold was 100 °C·min^{-1}.

2.4 Microstructure characterization

In order to determine the distribution of SiC particles in Al-SiC composite, the microstructural characterization was conducted by means of a JEOL JSM-5600 scanning electron microscope (SEM, operated at 20 kV) in secondary electron mode. The samples with a dimension of 10 mm × 10 mm × 5 mm were sectioned from the ingots using a Buehler Isomet 1000 precision saw equipped with a diamond wafering blade. The cross section of the sample was ground by a grinding machine using a grinding disc with 30 μm diamond suspended in water lubricant, polished with 9, 6, 3 and 1 μm diamond suspended in water lubricant and etched in 0.5% HF acid solution for 13 s. To identify the microstructure of Al-SiC composite, two samples were sectioned from the bottom and the top of each *Φ*50 mm × 100 mm ingot. The volume fraction of SiC particles and primary solid Al particles was measured from 3 randomly-selected fields of view by image analysis using the Quantimet 520 Image Processing and Analysis System.

2.5 Performance testing

The *Φ*6 mm × 40 mm dog-bone-shaped tensile specimens were subjected to tensile tests at a constant strain rate of 5×10^{-4} s^{-1} on an Instron 8802 testing machine at room temperature. Six tests were conducted for each ingot and the average value was taken for analysis. The fractured surfaces were observed by SEM to understand the fracture behavior and mechanism.

3 Results and discussion

3.1 Distribution of SiC particles

Figures 4–6 show the microstructures of the Al-4.25vol.%SiC ingots cast from the Al-SiC slurry at stirring speeds of 300, 600 and 900 r·min^{-1}. The phases circled by the oval dash lines are primary solid Al phase, and the nubbly phase is SiC particle, which shows an island ditribution in the matrix. It can be seen that the distribution of the SiC particles at the top is similar with that at the bottom of the Al-4.25vol.%SiC ingot with the stirring speed of 300 and 600 r·min^{-1} (Figs. 4 and 5). While the

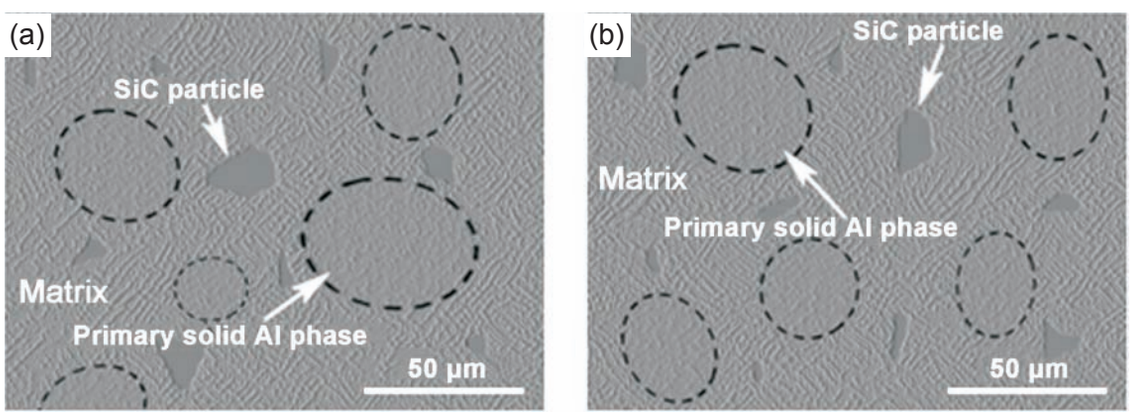

Fig. 4: Microstructures of ingot prepared with strring speed of 300 r·min^{-1}: (a) at bottom; (b) at top

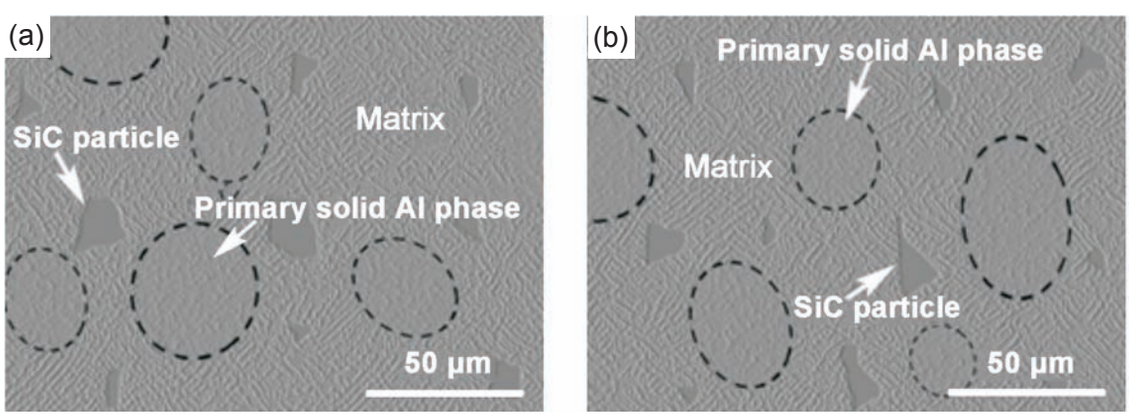

Fig. 5: Microstructures of ingot prepared with strring speed of 600 r·min^{-1}: (a) at bottom; (b) at top

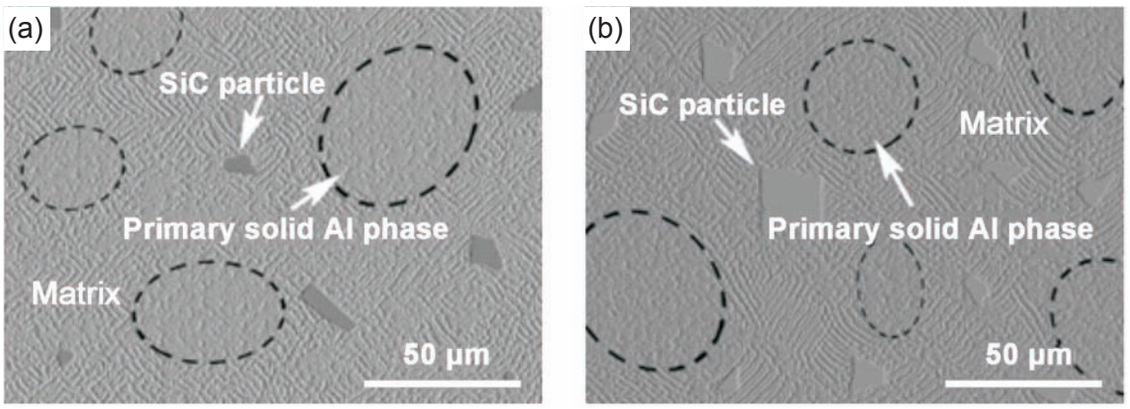

Fig. 6: SEM microstructures of ingot prepared with strring speed of 900 r·min^{-1}: (a) at bottom; (b) at top

distribution of the SiC particles at the bottom (Fig. 6a) is sparser than that at the top (Fig. 6b) of the Al-4.25vol.%SiC ingot under the stirring speed of 900 r·min^{-1}.

Figure 7 displays the SiC volume fractions in the top and bottom cross sections of ingots under different stirring speeds. When the stirring speeds are 300 and 600 r·min^{-1}, the differences between the SiC volume fraction in the top cross section and that in the bottom cross section of the Al-4.25vol.%SiC ingot are both ~0.04vol.%, and those are so small that the distributions of SiC particles can be considered as the homogeneous. When the stirring speed is 900 r·min^{-1}, the SiC volume fraction (5.44vol.%) in the top cross section is much greater than that in the bottom cross section (3.06vol.%) of the Al-4.25vol.%SiC ingot. This reveals that the distribution of SiC particles is uneven.

The distribution of SiC particles in the Al-4.25vol.%SiC ingot is predominantly determined by the distribution of SiC particles in the slurry during stirring and the settling of SiC particles during casting. In this work, the density of the Al foil

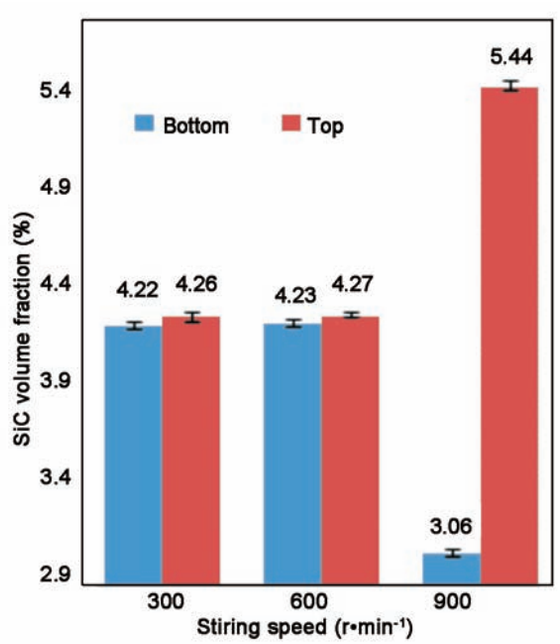

Fig. 7: SiC volume fraction in cross section of ingots versus stirring speed

are greater than that of the Al matrix liquid and the SiC particles wrapped in it tend to settle at the bottom of the crucible under the interfacial tension of Al matrix liquid after the melting of Al foil. In the electromagnetic-mechanical stirring, the blade on the inner wall of crucible has a horizontal tilt angle of 25°. It can change the horizontally circumferential movement of slurry to a movement along the blade surface and generate a suitable upward movement of slurry (Fig. 3). This upward movement can continuously drive the SiC particles to move upwardly. However, the horizontally circumferential movement of slurry in the stirring can also drive the SiC particles to move from the center to the periphery of the crucible under the action of centrifugal force. When the stirring speed is high (such as 900 r·min^{-1}), too many SiC particles cluster at the periphery of crucible, this can results in a uneven distribution. As for the stirring speeds of 300 and 600 r·min^{-1}, the turbulent action at the edges of blade can eliminate the clustering of SiC particles at the periphery of the crucible. Therefore, the SiC particles can disperse evenly. The uniform distribution of SiC particles in Al-SiC slurry under the stirring speed of 600 r·min^{-1} also can be certified by the simulation using FLUENT software. It can be seen that the volume fraction of SiC particles is very near 4.25vol% within the whole crucible (Fig. 8).

Figure 9 shows the microstructures of the ingot for comparison (prepared at the stirring temperature of 635 °C and the stirring speed of 600 r·min^{-1}) which forms about 5vol.% volume fraction of primary solid Al particles according to the image analysis. It can be seen that a large number of SiC particles settle at the bottom of ingot. In the present work, the stirring temperature is 620 °C and the volume fraction of primary solid Al particles is about 20vol.% according to the image analysis. Under this high viscosity of slurry, the primary solid Al particles can entrap the SiC particles completely before solidification of slurry in the permanent mold. Thus the settling of SiC particles is avoided during casting and the uniform distribution of SiC particles can be realized in the ingots (Fig. 5).

During casting, the settling of SiC particles is influenced by the viscosity and solid particles according to the Stokes equation[10, 17]. As for the Al-SiC slurry with too small volume fraction of primary solid Al particles, the viscosity of slurry is too low and the limited primary solid Al particles cannot entrap

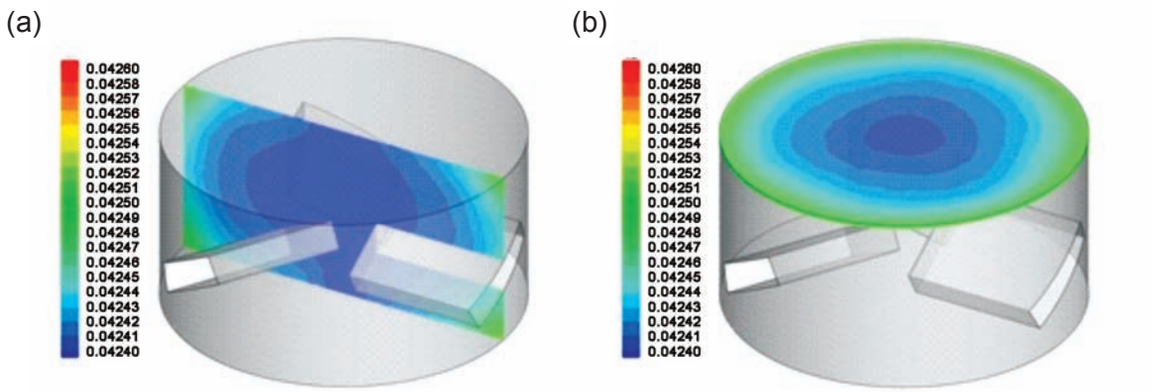

Fig. 8: Distribution of SiC particles in slurry simulated by FLUENT software: (a) contour of SiC volume fraction along axis of crucible; (b) contour of SiC volume fraction on top of crucible (the color scale demonstrates the volume fraction of SiC particles).

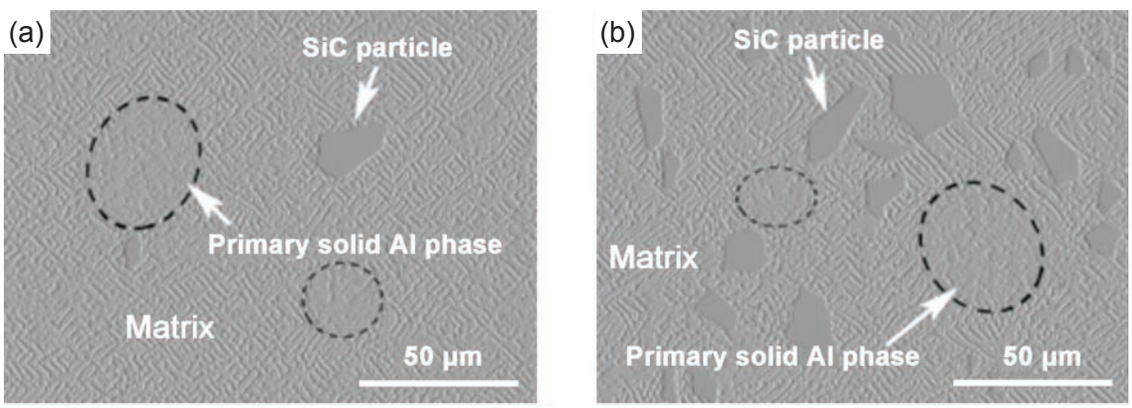

Fig. 9: Microstructures of ingot for comparison which from about 5 vol.% volume fraction of primary solid Al particles: (a) at top; (b) at bottom

the SiC particles fully. Thus the settling of SiC particles cannot be restricted during casting.

3.2 Performance

Figure 10 displays the typical stress-strain curves of the Al matrix and the homogeneous Al-4.25vol.% SiC composite. Table 1 exhibits the relative tensile strength improvements [(Tensile strength of composite – Tensile strength of matrix)/ Tensile strength of matrix] of various stir-casting Al-SiC composites with similar contents (4vol.% or 5vol.%) of SiC particles prepared by other researchers [15,18,19]. From Table 1, it can be seen that the relative tensile strength improvement (51.2%) of the resulting Al-SiC composite in the present work is much greater than those of the other stir-casting Al-SiC composites with a similar content of SiC particles (6.1%, 10.8%, 30.9 %).

In Al-SiC composite, the SiC particles is hard enough to restrict the plastic flow of Al matrix and create a strengthening effect on the Al matrix [19]. Especially, the homogeneous distribution of SiC particles can avoid the weakening of particle clustering [20]. Thus the Al-SiC composite with the homogeneous distrbution of SiC can possess an excellent tensile strength.

In addition, the porosity in the Al-SiC composite can cause the early crack initiation by decreasing the effective load-carrying area and inducing the local stress concentration under

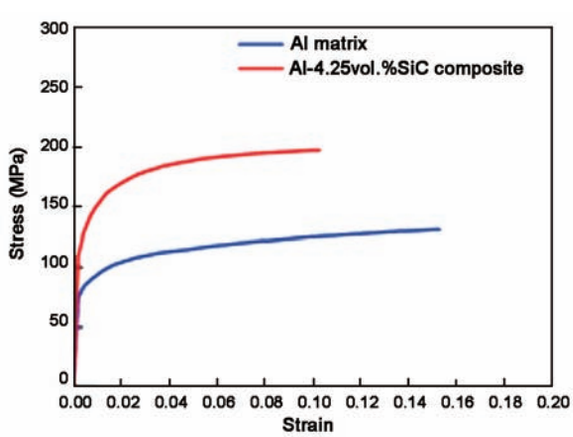

Fig. 10: Typical stress-strain curve of Al matrix and homogeneous Al-4.25vol.% SiC composite

the action of tensile load [21]. In the present work, the threaded cover and the sealing plug keep the air standing out of the crucible. Consequently, no air is entrapped in the ingots (Figs. 4–6). Table 2 shows the calculated porosity (P) of the ingots from the following equation:

$$P = 1 - \frac{\rho_{ac}}{\rho_{th}} = 1 - \frac{\rho_{ac}}{\rho_{Al}(1-V_{SiC})+\rho_{SiC}V_{SiC}} \quad (1)$$

where ρ_{ac} (10^3 kg·m^{-3}) is the actual density of the composite

measured by the Archimedian principle, ρ_{th} (10^3 kg·m^{-3}) is the theoretical density of composite calculated using the mixture rule, ρ_{Al} (10^3 kg·m^{-3}) is the density of Al matrix alloy, ρ_{SiC} (10^3 kg·m^{-3}) is the density of SiC and V_{SiC} is the volume fraction of SiC particles. It can be seen that the porosity of the ingot mainly resulting from the residual solidification shrinkage of slurry is rather small (< 0.04vol.%) [22–23]. Therefore, the homogeneous distrbution of SiC in the Al-SiC composite can enhance the tensile strength of Al matrix greatly.

Figure 11 shows the typical SEM fractographs of the Al matrix and Al-4.25vol.%SiC composite. In the fracture surface of Al matrix (Fig. 11a), the typical ductile fracture is exhibited. The dimples resulted from the void nucleation and the subsequent coalescence by strong shear deformation are apparent [24]. In the fracture surface of Al-4.25vol.% SiC composite (Fig. 11b), both ductile and brittle natures of the fracture behavior are shown. For SiC particles, brittle fracture as a result of work-hardening and high stress concentration is predominant. This illustrates the firm bonding between SiC particles and Al matrix and further explains the reinforcing mechanism of the Al-4.25vol.% SiC composite.

Table 1: Tensile properties of Al matrix and Al-4.25vol.%SiC composite

Sample	Processing method	Component	Tensile strength (MPa)	Relative tensile strength improvement
1[pw]	Stir casting	Al-1.5wt%Si matrix	131 ± 3	51.2%
		Al-4.25vol.%SiC composite	198 ± 3	
2[15]	Stir casting	A356 matrix	180	6.1%
		Al-5wt.%SiC composite	191	
3[18]	Stir casting	Commercial pure Al matrix	67.7	10.8%
		Al-5vol.%SiC composite	75	
4[19]	Stir casting	Al6061 matrix	123	30.9%
		Al-4wt.%SiC composite	161	

Relative tensile strength improvement = (Tensile strength of composite - Tensile strength of matrix) / Tensile strength of matrix

Table 2: Calculated porosity of ingots

Sample	ρ_{ac} (10^3 kg•m^{-3})	ρ_{th} (10^3 kg•m^{-3})	Porosity (vol. %)
Ingot under 300 r·min^{-1}	2.7038 ± 0.0002	2.7048	0.037 ± 0.006
Ingot under 600 r·min^{-1}	2.7040 ± 0.0002	2.7048	0.030 ± 0.006
Ingot under 900 r·min^{-1}	2.7039 ± 0.0002	2.7048	0.033 ± 0.006

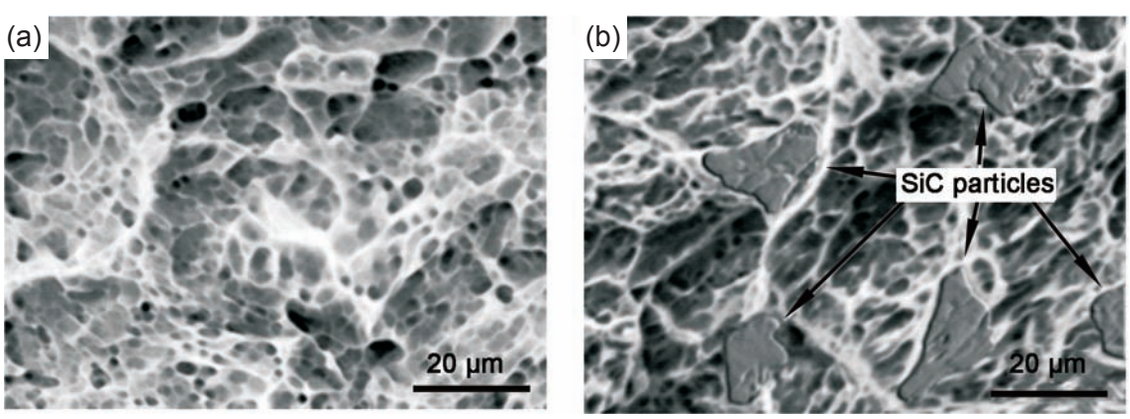

Fig. 11: Typical SEM fractograph of Al matrix (a) and Al-4.25vol.%SiC composite (b)

4 Conclusions

In the semisolid stir casting of Al-4.25vol.% SiC composite, the homogeneous composite could be obtained in a permanent mold using the Al-SiC slurry prepared by the electromagnetic-mechanical stirring under 300–600 r·min^{-1} in the crucible with blades tilting 25 ° horizontally at 620 °C.

The distribution of the SiC particles at the top is similar with that at the bottom of the Al-4.25vol.%SiC ingot with the electromagnetic stirring speed of 300 and 600 r·min^{-1}. In addtion, when the stirring speeds are 300 and 600 r·min^{-1}, the differences between the SiC volume fraction in the top cross section and that in the bottom cross section of the Al-4.25vol.%SiC ingot are both ~0.04vol.%, and those are so small that the distributions of SiC particles can be considered as the homogeneous. This is because the horizontally tilting blades could realize the upward movement of SiC particles and could eliminate the clustering of SiC particles at the periphery of the crucible at the stirring speed of 300–600 r·min^{-1}. The high viscosity and the primary solid Al particles of the slurry stirred at 620 °C could entrap the SiC particles completely before solidification of the slurry in the permanent mold and the settling of SiC particles was avoided during casting.

The tensile strength of the Al matrix could be enhanced by

51.2% due to the uniformly distributed of SiC particles in the resulting Al-4.25vol.% SiC composite.

The porosity of the composite mainly resulting from the solidification shrinkage of slurry was less than 0.04vol.% because the threaded cover screwed into the threaded crucible and the sealing plug on the threaded cover could keep the air standing out of the crucible.

References

[1] Xie B, Wang X G, Hua X H, et al. Process and Performance of β-SiCp/Al Prepared by Bottom-vacuum Pressureless Infiltration. Rare Metal Mat. Eng., 2014, 43(9): 2089–2094.

[2] Mosleh-Shirazi S, Akhlaghi F, Li D Y. Effect of SiC Content on Dry Sliding Wear, Corrosion and Corrosive Wear of Al/SiC Nanocomposites. Trans. Nonferrous Met. Soc. China, 2016, 26(7): 1801–1808.

[3] Khodabakhshi F, Gerlich A P, Švec P. Fabrication of a High Strength Ultra-fine Grained Al-Mg-SiC Nanocomposite by Multi-step Friction-stir Processing. Mater. Sci. Eng. A, 2017, 698: 313–325.

[4] Teng F, Yu K, Luo J, et al. Microstructures and Properties of Al−50%SiC Composites for Electronic Packaging Applications. Trans. Nonferrous Met. Soc. China, 2016, 26(10): 2647–2652.

[5] Si Y Q, You Z Y, Zhu J X, et al. Microstructure and Properties of Mechanical Alloying Particles Reinforced Aluminum Matrix Composites Prepared by Semisolid Stirring Pouring Method. China Foundry, 2016, 13(3): 176–181.

[6] Fathy A, Sadoun A, Abdelhameed M. Effect of Matrix/reinforcement Particle Size Ratio (PSR) on the Mechanical Properties of Extruded Al−SiC Composites. Int. J. Adv. Manuf. Tech., 2014, 73(5-8): 1049–1056.

[7] Vijayavel P, Balasubramanian V. Effect of Pin Profile Volume Ratio on Microstructure and Tensile Properties of Friction Stir Processed Aluminum Based Metal Matrix Composites. J. Alloy. Comp., 2017, 729: 828–842.

[8] Wu S S, Yuan D, Lü S L, et al. Nano-SiCP Particles Distribution and Mechanical Properties of Al-matrix Composites Prepared by Stir Casting and Ultrasonic Treatment. China Foundry, 2018, 15(3): 203–209.

[9] Previtali B, Pocci D, Taccardo C. Application of Traditional Investment Casting Process to Aluminium Matrix Composites. Compos. Part A, 2008, 39(10): 1606–1617.

[10] Naher S, Brabazon D, Looney L. Development and Assessment of a New Quick Quench Stir Caster Design for the Production of Metal Matrix Composites. J. Mater. Process. Tech., 2004, 166(3): 430–439.

[11] Amirkhanlou S, Niroumand B. Synthesis and Characterization of 356-SiCp Composites by Stir Casting and Compocasting Methods. Trans. Nonferrous Met. Soc. China, 2010, 20(s3): s788–s793.

[12] Ureña A, Martínez E E, Rodrigo P, et al. Oxidation Treatments for SiC Particles Used as Reinforcement in Aluminium Matrix Composites. Compos. Sci. Technol., 2004, 64(12): 1843–1854.

[13] Singh S, Pal K. Influence of Surface Morphology and UFG on Damping and Mechanical Properties of Composite Reinforced with Spinel $MgAl_2O_4$-SiC Core-shell Microcomposites. Mater. Charact., 2017, 123: 244–255.

[14] León C A, Drew R A L. The Influence of Nickel Coating on the Wettability of Aluminum on Ceramics. Compos. Part A, 2002, 33(10): 1429–1432.

[15] Vanarotti M, Shrishail P, Sridhar B R, et al. Study of Mechanical Properties & Residual Stresses on Post Wear Samples of A356-SiC Metal Matrix Composites. Procedia Materials Science, 2014, 5(3873): 873–882.

[16] Hashim J, Looney L, Hashmi M S J. The Enhancement of Wettability of SiC Particles in Cast Aluminium Matrix Composites. J. Mater. Process. Technol., 2001, 119(1-3): 329–335.

[17] Heidary D S B, Akhlaghi F. Theoretical and Experimental Study on Settling of SiC Particles in Composite Slurries of Aluminum A356/SiC. Acta Mater., 2011, 59(11): 4556–4568.

[18] Arab M S, Mahallawy N E, Shehata F, et al. Refining SiCp in Reinforced Al-SiC Composites Using Equal-channel Angular Pressing. Mater. Design, 2014, 64: 280–286.

[19] Lokesh T, Mallikarjun U S. Mechanical and Morphological Studies of Al6061-Gr-SiC Hybrid Metal Matrix Composites. Applied Mechanics and Materials, 2015, 813-814: 195–202.

[20] Mazahery A, Shabani M O. Microstructural and Abrasive Wear Properties of SiC Reinforced Aluminum-based Composite Produced by Compocasting. Trans. Nonferrous Met. Soc. China, 2013, 23(7): 1905–1914.

[21] Li C S, Ellyin F, Koh S, et al. Influence of Porosity on Fatigue Resistance of Cast SiC Particulate-reinforced Al-Si Alloy Composite. Mater. Sci. Eng. A, 2000, 276(1-2): 218–225.

[22] Ilegbusi O J, Yang J J. Porosity Nucleation in Metal-matrix Composites. Metall. Mater. Trans. A, 2000, 31(8): 2069–2074.

[23] Podymova N B, Karabutov A A. Combined Effects of Reinforcement Fraction and Porosity on Ultrasonic Velocity in SiC Particulate Aluminum Alloy Matrix Composites. Compos. Part B, 2017, 113: 138-143.

[24] Song M. Effects of Volume Fraction of SiC Particles on Mechanical Properties of SiC/Al composites. Trans. Nonferrous Met. Soc. China, 2009, 19(6): 1400–1404.

This work was financially supported by the Beijing Natural Science Foundation (No. 2162036).